



Ecole Polytechnique Federale de Lausanne
Biorobotics Laboratory

SEMESTER PROJECT

Unconventional gait exploration with Pleurobot. The side-winding gait

Student
Olguța Robu

Advisers
Prof. Auke Jan Ijspeert
Kamilo Melo
Tomislav Horvat

Lausanne, 2015

Contents

List of Figures	ii
1. Introduction	1
2. Theoretical Background	2
2.1. The Side-Winding Gait	2
2.1.1. Visual Description	2
2.1.2. Mathematical Description	3
2.1.3. Key Aspects in The Motion	4
Synchronization	4
Amplitudes	5
Ground Contact Surface	5
Ground Contact Tracks	5
Conical Side-winding	6
2.2. Advantages of Side-Winding	7
3. Side-Winding From Snake to Salamander Robots	8
3.1. Porting Side-winding to Pleurobot	8
3.2. Workspace	9
4. Problem To Be Solved	11
4.1. Problem Statement	11
4.2. Keys to Solutions	11
5. Proposed Implementations	12
5.1. Using The Limbs to Replace The Vertical Wave Made by Snakes	12
5.2. Using a State Machine	13
5.2.1. The Method	13
5.2.2. Tests	15
5.3. Have a " <i>Spine-Triggered</i> " Motion of The Limbs	17
5.3.1. The Method	17
5.3.2. Tests	18
5.4. Stabilize the Girdles and Compute the Joints Angles from Wave Functions	21
5.4.1. The Method	21
5.4.2. Tests	22
5.5. Comparing The Methods	23
5.6. Practical Experiments	25
6. Conclusions and Further Work	26
Appendices	30
A. Notations And Acronyms	30

1. Introduction

To begin with, the goal of this project is the exploration of an unconventional snake-inspired gait for salamanders which involves both simulations and tests on the real platform. The side-winding is a type of locomotion specific to sand-snakes that has already been successfully implemented on modular snake robots like Lola-OP.

Why is it interesting to implement on a salamander-inspired (*Pleurodeles walt*) quadruped robot a gait that is specific to sand-snakes? That is because it has a number of advantages that make it desirable in any robot: terrain-wise, it has a big footprint on the ground which leads to improved stability and static, not sliding friction which results in minimal frictional resistance from its environment. In addition, it is useful on granular terrain, where the ground is not generating enough reaction forces needed for other motions. Energetically-wise, since there is only static friction, there is no waste of energy on resistant forces. Low energy is used for the vertical motion, which is very small. Performance-wise it is described by big speed and reduced wear caused by friction.

Knowing all these advantages, proved for instance on Lola-OP, it is interesting to try and port them to other robots. What should be done for that? Unfortunately, in the Pleurobot, the spine does not have all the capabilities of a real snake and not even of Lola-OP, therefore, the motion has to be rethought in such a way that the limbs have to take a part of the spine's task in terms of vertical motion. That is why, part of the project's focus is to find an effective way to use the Pleurobot's 4-DOFs limbs to produce the vertical wave effect present in the snake's spine.

The first steps towards implementing side-winding on Pleurobot are made by establishing a working methodology. There are several hypotheses that are to be tested. One of them is the fact that all the spine, including the tail, should be used. Another assumption is that, unlike the Lola-OP, Pleurobot will not be able to maintain a strictly lateral displacement, but due to tail friction and morphological asymmetries the direction and orientation might deviate.

The outline of this paper is as follows. In Chapter 2, some theoretical aspects concerning the side-winding gaits in desert snakes' locomotion are introduced. With them, some key elements are identified and discussed leading to the main advantages of this are derived. In Chapter 3, the main research topic is defined. A general goal will be stated, and further on, more focused questions are to be addressed. In Chapter 4 a clear problem statement is given and the possible solutions are proposed. Following up, Chapter 5 presents the different implementation stages, from proposed trajectories and state design patterns to robot implementation and their outcomes. Finally some conclusions are presented and directions for further potentially fruitful research are suggested.

2. Theoretical Background

2.1. The Side-Winding Gait

2.1.1. Visual Description

In the literature (Burdick et al; 1993 Hatton et al; 2010 Gong et al; 2012 Marvi et. al.; 2014) an important element that describes the side-winding motion are the *Ground Contact Tracks (GCT)*. A side-winder snake moving uniformly on a sand-like surface, has 2 or maximum 3 segments of the body touching the ground at a time. They are called *Ground Contact Segments (GCS)* and are in *static (not sliding) contact with the ground*, such that the snake constantly lifts and lays portions of its body to redistribute weight in the direction of locomotion. The portions of the body that are in the air are called *Arch Segments (AS)*.

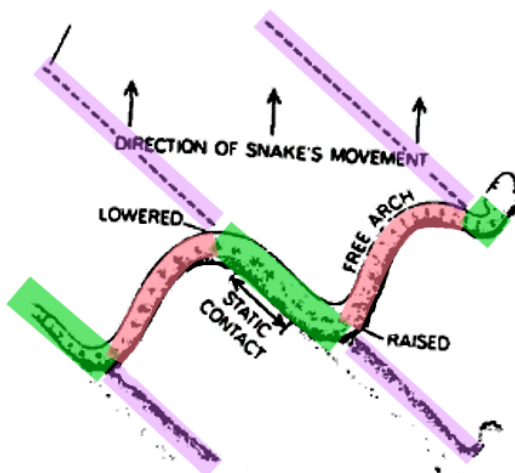


Figure 2.1.: The image illustrates a snake performing the sand-winding motion. The purple lines are called Ground Contact Tracks (GCT) and are left on the locomotion surface by the Ground Contact Segments (GCS) (in green). The red portions of the snake are called Arch Segments (AS). Image source: Burdick et al; 1993

The side-winding motion seems to be very complex, but experimental proof show that it can be decomposed in identical cycles of simpler movements, in the case of uniform displacement, as follows:

- One cycle can be considered as beginning in the moment when the snake's head (actually not the head, but a point that is on the ground) lifts from a GCT, until he lifts his head from the following GCT;

- After the snake lifts its head from a GCT, it sequentially lifts segments of its body behind the head, until the AS containing the head reaches a certain length that is dependent on a wave length that will be introduced later;
- Then, a point from behind its head, is put on to the ground; At that point, a new CGT begins and the portion behind that point is propagated along the new CGT;
- The arch segment between that point and the head will stay at rest, while the rest of the body is propagated along the GCT;

2.1.2. Mathematical Description

The macroscopic effect of the side-winding motion can be described in various ways, by describing the trajectory of each point of the snake's backbone curve with *shape functions* (Burdick et al; 1993) or by employing resemblances with simpler motions. For instance, a side-winder can be abstracted as a circular helix (or a cylinder) that is rolling on a surface (Hatton et al; 2010), or, for changing the heading, the motion can be seen as a rolling cone (Gong et al; 2012).

An analogy that completely describes the side-winding gait and offers a straightforward solution for implementing the motion on snake-robots is the *wheel-wave decomposition* (Melo; 2015) illustrated in figure (2.2).

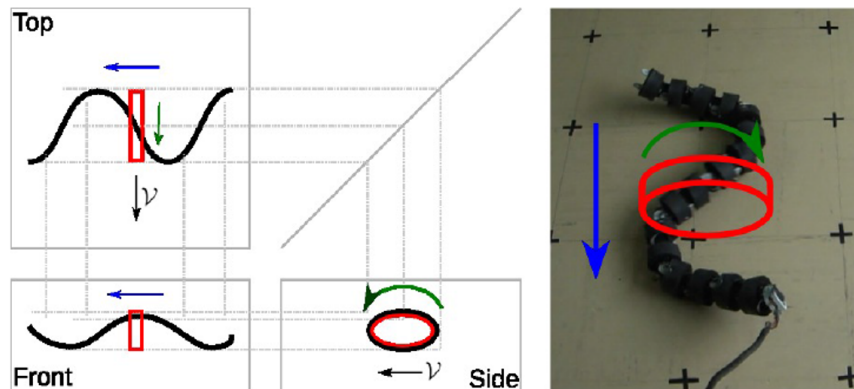


Figure 2.2.: Top perspective-high amplitude wave , front perspective w.r.t the direction of displacement-low amplitude wave, and lateral perspective - ellipsoidal wheel. Image source: Melo; 2015

As figure 2.2 shows, the wheel-wave formalism presents the motion as a composition of two waves and an ellipsoidal rolling wheel. In fact, the ellipsoidal wheel is only performing a fictive roll, since in practice, the robots and the real snake do not perform a roll motion, but only maintain the body in a wheel shape, as seen from the "Side" perspective in figure 2.2.

Therefore, the side-winding motion can be implemented using only two sinusoidal waves. One wave is vertical, is meant to reduce the contact with the ground and has a small amplitude. The second wave is vertical, has a large amplitude and has the purpose to produce the horizontal displacement of the snake's body. For a modular snake robot, the two wave functions can be represented by formula 2.1.

$$\Theta(n, t) = \begin{cases} A_o \sin(\frac{n}{\lambda} + \omega t), n = \text{odd} \\ A_e \sin(\frac{n}{\lambda} + \omega t + \delta), n = \text{even} \end{cases} \quad (2.1)$$

where:

- $\Theta(n, t)$ is the angle of module n
- A_o is the amplitude of the odd modules
- A_e is the amplitude of the even modules
- n is the number of each module
- λ is the wavelength of the two waves
- ω is the frequency of the waves
- t is the time
- δ is a phase shift

This function is an extension of the Hirose's *serpenoid curve* (Hirose; 2009).

2.1.3. Key Aspects in The Motion

Synchronization

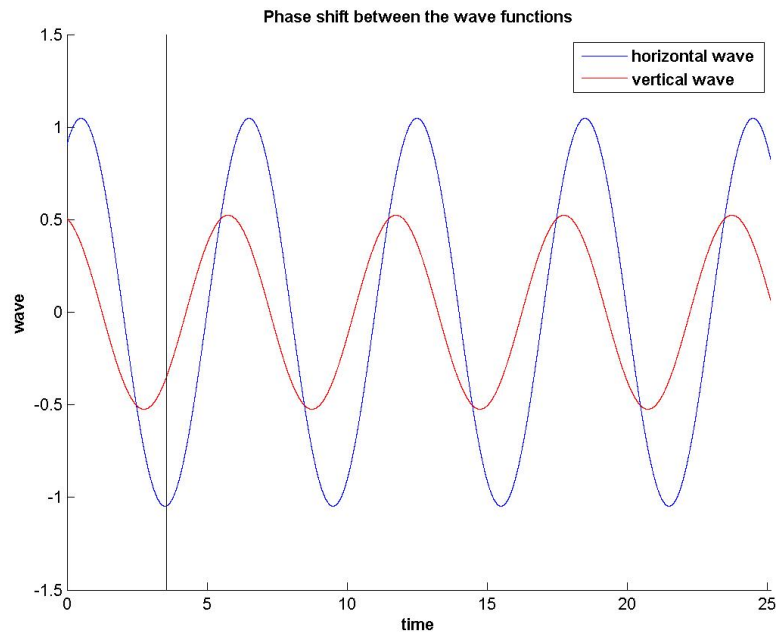


Figure 2.3.: Illustration of the timing of the wave functions. The vertical line is placed at $\pi/4$ after the minimum value of the vertical wave (red color) . At the same point the horizontal wave (blue color) has a minimum value and starts to grow

Shortly after a module of the snake is lifted from a GCT, it also starts an horizontal motion in the direction of the displacement. This means that the two waves are synchronized ($\frac{n}{\lambda} + \omega t$), with an optimal phase shift $\delta = \pi/4$ (Melo; 2015), as figure 2.3 illustrates. That is done so that each lifted portion is propagated a maximum distance on the direction of displacement until it is placed again on the ground.

Amplitudes

The robot does a big displacement while making little lift from the ground. This translates into a small amplitude vertical wave and high amplitude horizontal wave ($A_o > A_e$). Image 2.2 illustrates the visual effect of the two waves: frontally with respect to the direction of motion (the bottom fo the figure), the amplitude of the vertical wave is emphasized using a red rectangle; the top perspective offers (top of the figure) a view of the horizontal wave which, as the red rectangle shows, has a larger amplitude.

This key feature withholds part of the side-winding's success. That is first of all, that with the large amplitude horizontal wave a big speed of the displacement is achieved. Then, having a low amplitude vertical wave, little energy is consumed for it.

Ground Contact Surface

When using a modular snake robot, there are a few modules on the ground; most of them are in the air "flying". In other words, the body length in contact with the ground at a certain instant, has to be small, so that enough length is left to perform the horizontal wave propagation (displacement).

If the wave functions in formula 2.1 are considered, this small contact property is withheld in the wavelength of the two waves: it has to be $\lambda = \frac{n_{wave}}{2\pi}$, when n_{wave} is the number of modules in a complete wave. For example for a 16DOF snake robot λ is $3/\pi$ or $6/\pi$ (Melo; 2015).

Ground Contact Tracks

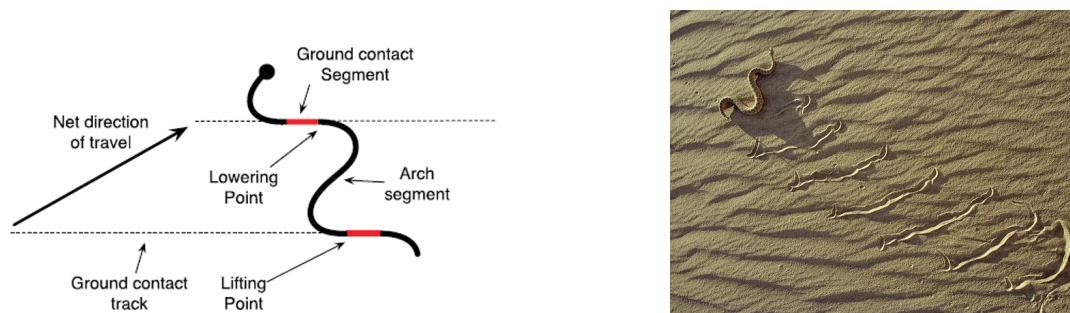


Figure 2.4.: Ground Contact Tracks. Image source: Gong et al, 2012 and http://animals.nationalgeographic.com/animals/photos/rattlesnakes//sidewinder-rattlesnake_5864_00x450.jpg

Empirical observations show that while a snake side-winds, it leaves behind (in the case of straight uniform motion) straight, parallel GCTs, as figure 2.4 shows. This happens

because the two mentioned amplitudes are constant in time and equal for all the odd or even modules ($A_o = \text{constant}$ and $A_e = \text{constant}$).

As **Burdick et al; 1993** mention, the fact that having straight parallel GCTs imply straight uniform movement, can be used if turning is desired.

Hence, as images 2.5, 2.6 and 2.7 show, turning implies changing the shape of the GCTs, or changing the orientation. In figure 2.5, turning is performed by placing the head on a new GCT, at a different position on the length of the GCT. In figure 2.6, the turn is performed by making a GCT that is not parallel with the previous ones. As well, in figure 2.7 the GCTs are not straight any more, but circular, which results in turning. This is not highly relevant for this project, but gives some insight on the fact that with side-winding turning can also be performed.

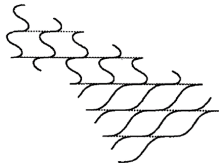


Figure 2.5.: Head placement

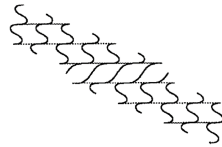


Figure 2.6.: Skew GCTs

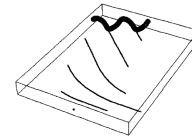


Figure 2.7.: Curvilinear GCTs

Images source: **Burdick et al; 1993**

Conical Side-winding

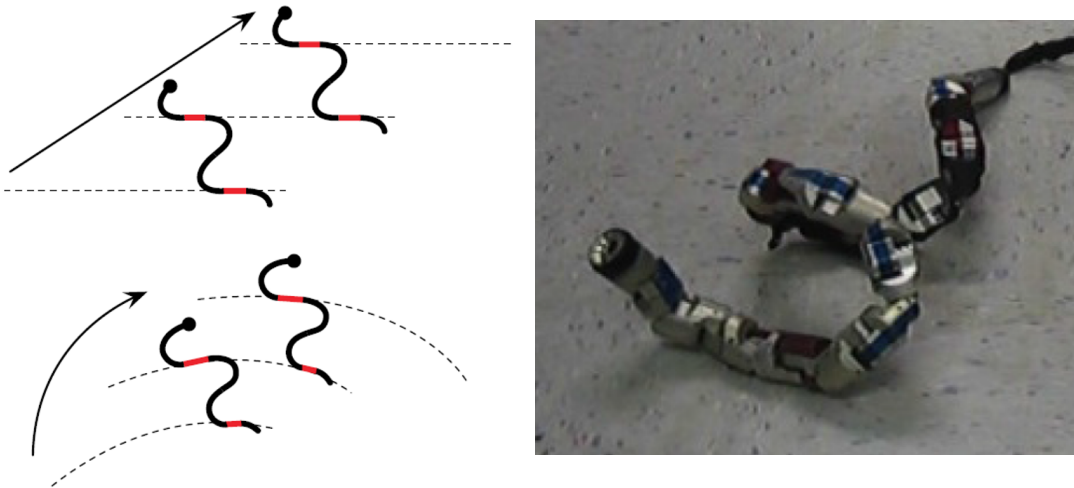


Figure 2.8.: Conical side-winding
Images source: Gong et al, 2012

As illustrated in the previous paragraph, turning can be done by curvilinear GCTs. According to **Gong et al; 2012** One way of obtaining such a profile is to lay the snake's spine on a cone's surface, instead of a cylinder, such that:

- the taper of the cone gives the turning rate;
- the backbone's distribution on the cone's surface affects the lateral stability of the robot.

One way of obtaining conical side-winding while considering the equation 2.1 may be, by considering variable amplitudes across modules: $A_e = A_e(n)$ and $A_o = A_o(n)$.

2.2. Advantages of Side-Winding

Considering all of the above key features, there are some important advantages that can be derived from them.

First of all, by having only static, not sliding friction with the environment, there is not a waste energy on resistant forces. As well, the wear caused by friction is reduced. Then, having a large amplitude horizontal wave and a small amplitude vertical wave, there is a big footprint of the snake on the ground, which means it has improved stability. As well, the energy used for the vertical motion is very small, while the resulting speed is very big. The contact with the ground in two or three points equally distanced which makes suitable on loose or granular terrain that gives small reaction forces.

To sum up the advantages, they are:

- Terrain-wise
 - Big footprint of the snake on the ground \Rightarrow improved stability
 - Static, not sliding friction \Rightarrow minimal frictional resistance from its environment
 - Useful on granular terrain where the ground is not generating enough reaction forces needed for other motions
 - Contact reaction forces are distributed over several GCS \Rightarrow improved stability (Burdick et al, 1993)
- Energetically-wise
 - Only static friction \Rightarrow not wasting energy on resistant forces
 - Low energy used for the vertical motion, which is very small
- Performance-wise
 - Big speed
 - Reduced wear caused by friction

As a result, given the appropriate robot, side-winding can represent a very convenient solution for displacement on granular terrain or on inclined surfaces with undulant type robots. That is why, further on the focus will be used on producing and testing a similar *side-winding-like* gait implementable on the present body of Pleurobot.

3. Side-Winding From Snake to Salamander Robots

IN this chapter the main research topic is defined. To begin with, a general goal will be stated, and further on, more focused questions are to be addressed.

3.1. Porting Side-winding to Pleurobot

Side-winding has lots of advantages, of which, reminding: functions on granular terrain, big speed, reduced wear, little energy wasted for the vertical motion. Therefore, it is convenient to port it to other platforms and verify if the gait maintains these advantages. Thus, the question that arises is: *What can be done, to port the side-winding to Pleurobot?*

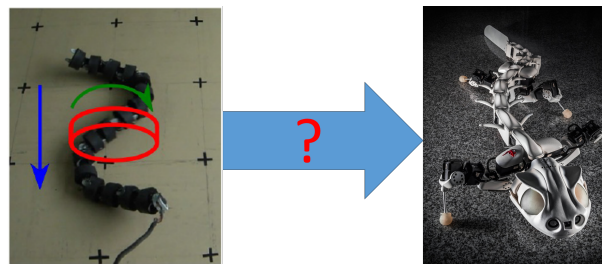


Figure 3.1.: How can the wave-wave-roll motion be implemented in Pleurobot?

To answer to the previous question, another one should be addressed first: What are the common and what are the distinct features between the two platforms? Lola-OP is 16 degrees of freedom (DOF) snake robot made of 16 one DOF actuators disposed on a single spine, capable of producing motion on the y (horizontally) and z (vertically) axis. Similarly, Pleurobot has an 11 DOF spine. However, it can only bend horizontally, on the y axis. In addition to the spine it also has 4 limbs, each one having 4 DOF which consist in roll, pitch, yaw, and elbow. Therefore, they can produce rotations around all axis.

Taking these structure particularities into account the solution that arises is to reproduce the snake's horizontal movement using the Pleurobot's spine and implement the snake's vertical motion using the 4 DOF limbs. The question has been now restricted to *How can the 4 DOF limbs be exploited, to produce the vertical wave effect present in the snake's spine?*

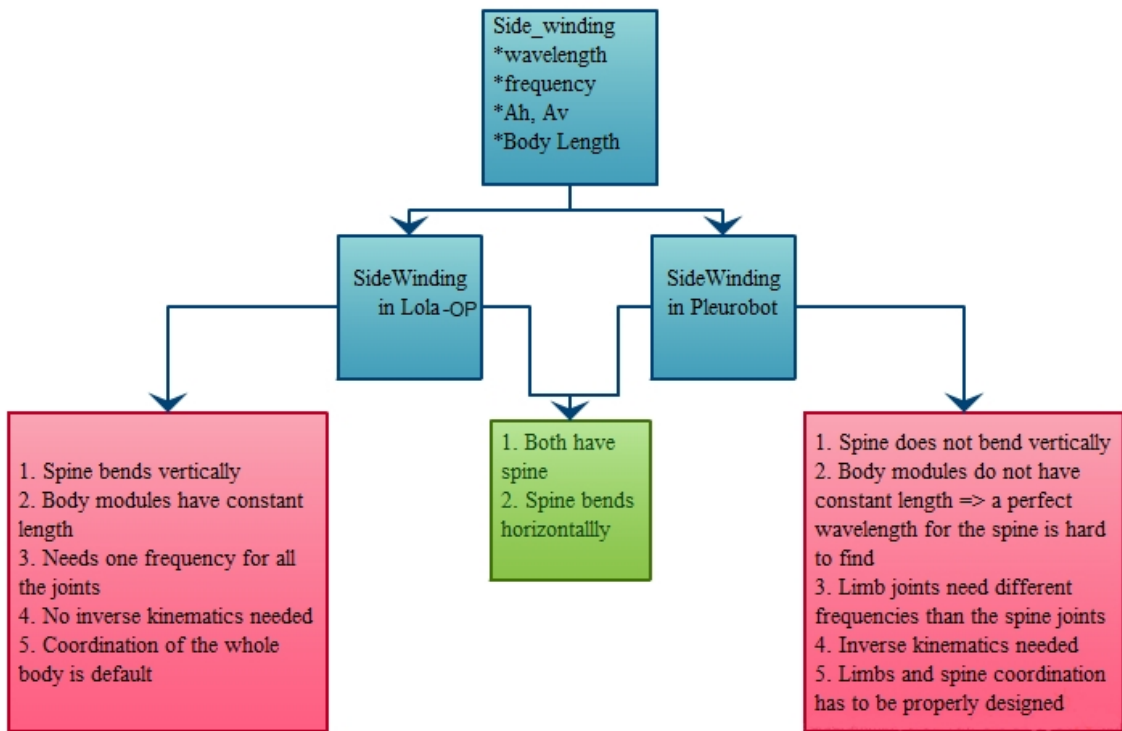


Figure 3.2.: How can the wave-wave-roll motion be implemented in Pleurobot?

3.2. Workspace

In order to test the success of the gait in the case of the salamander robot, a systematic approach is needed. First, the workspace for each limb was computed and it looks as shown in Figure 3.4 a) - d). Thus, the height at which the limbs have the biggest workspace (Figure 3.4 b)) could be determined and chosen for the implementation of the gaits.

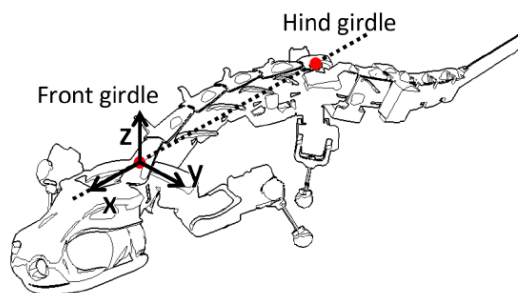
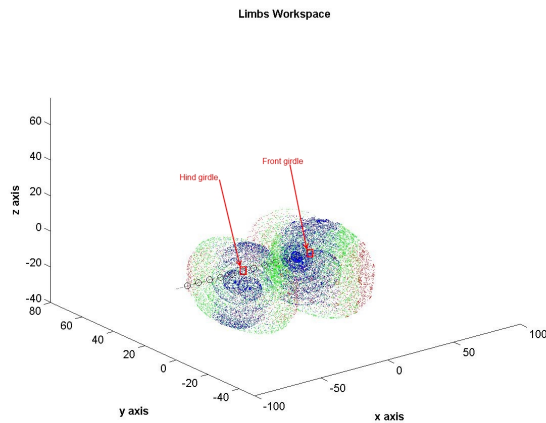


Figure 3.3.: Coordinates system

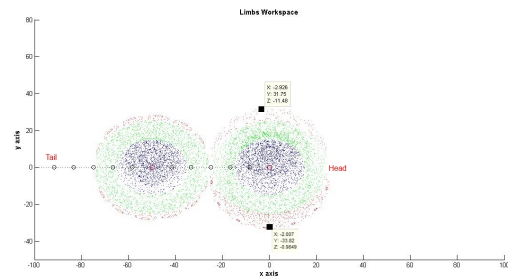
The coordinates system shall be considered as in the 3.3 image. Watching a top view of the salamander's workspace Figure 3.4 b), and taking into account that the workspace is colored in function of how big the workspace is on the x and y axis relative to the z axis, the z coordinate at which the limbs reach the largest surface can be identified. This

way the z coordinate at which the workspace is the biggest was found to be around -10 cm.

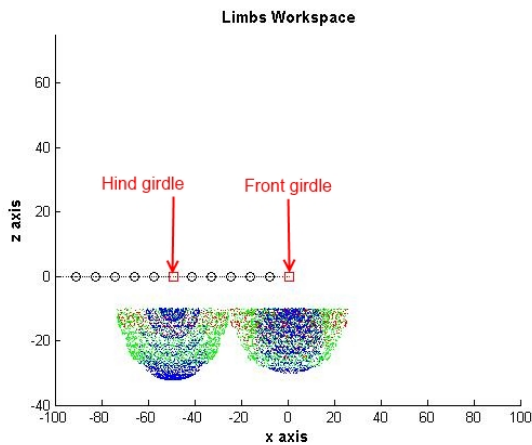
a) 3D perspective



b) Top



c) Side



d) Front

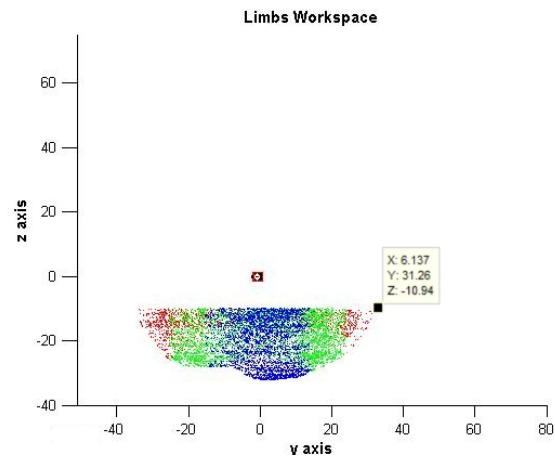


Figure 3.4.: The Pleurobot's limbs workspace: a) - a 3D view of all the workspace, b) a top view, c) Side and d) Front. The workspace is colored in function of how spread the workspace is on the x and y axis. More precisely in red the points with the distance w.r.t. the girdle greater than 25 cm, green the points with the distance w.r.t. the girdle between 15 and 25 cm, and in blue the points located at less of 15 cm on x and y w.r.t. the girdle.

After this step, a more mathematical problem statement has been formulated, following up with different designs solutions of the final implementation of the gaits. This step is detailed in Chapter 4. Then, the different types of gaits were implemented in Matlab. After that, Matlab and Webots simulations were carried out. And comparisons between gaits were considered in terms of speed and deviation from the desired trajectory. Finally, some gaits have been tested on the real platform as explained in the upcoming chapters.

4. Problem To Be Solved

IN this chapter a clear problem statement for the implementation of side-winding gait on the salamander-robot is given, and some possible solutions are proposed.

4.1. Problem Statement

The problem can be stated as follows. Given: the spine equation 2.1, the slope of the GCT, which, according to Melo; 2015 is equal to A_o , the distance between the GCTs, the contact points between the robot's body and the GCT and the vertical level (on z) at which the robot's body should be, with respect to the tip of the foot, which corresponds to the biggest workspace on x and y .

The requirement is to determine, the angles that need to be outputted to each of the four joints of Pleurobot (*Yaw, Pitch, Roll, Elbow/Knee*) of each limb, in order to obtain an overall lateral motion similar to side-winding in snakes, i.e. keep the body parts of the wave in contact with the virtual GCTs all the time aligned with it. The propagation of the wave must be concordant with the placement of exact the same parts of the wave no matter what parts of the body are executing it (Figure 2.4). This is the key of the construction of the GCTs. Part of the displacement is given by the wave implemented in the spine.

4.2. Keys to Solutions

To solve the stated problem, several different, but possibly complementary approaches were taken into consideration. Figure 4.1 outlines them.

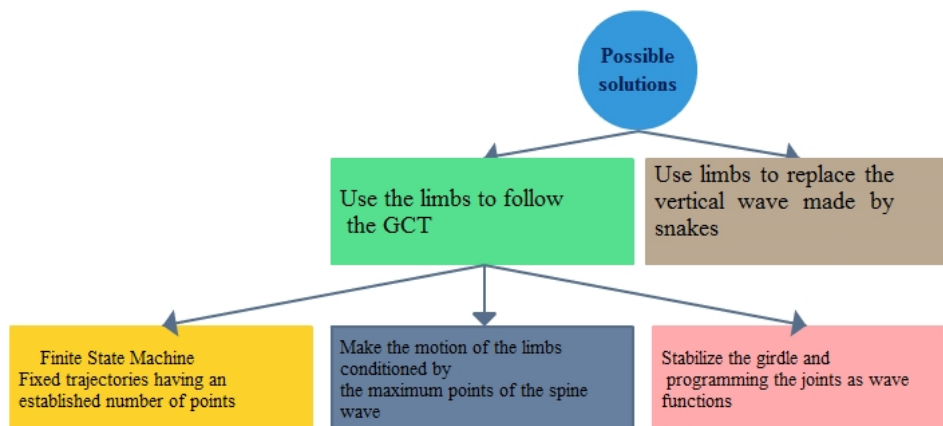


Figure 4.1.: The charts shows different approaches proposed in order to implement the side-winding gait on Pleurobot

5. Proposed Implementations

THIS chapter presents the different the approaches that were considered, some implementation solutions, simulations, practical trials and results.

Firstly, some ideas related to reproducing the vertical waves of snakes are introduced. Then, a method for implementing side-winding on Pleurobot based on a State Machine is presented and evaluated. Similarly, two more methods are presented and evaluated, one based on stepping when the spine’s wave is at maximum amplitude, and another one based on wave functions. Then, all the methods are compared.

5.1. Using The Limbs to Replace The Vertical Wave Made by Snakes

The first possible key to port the side-winding gait from the snake-robot to Pleurobot is to use the data that is known from the snakes: to produce the side-winding gait, their bodies make a horizontal wave and vertical wave, both propagated from head to tail, as explained in the previous chapters.

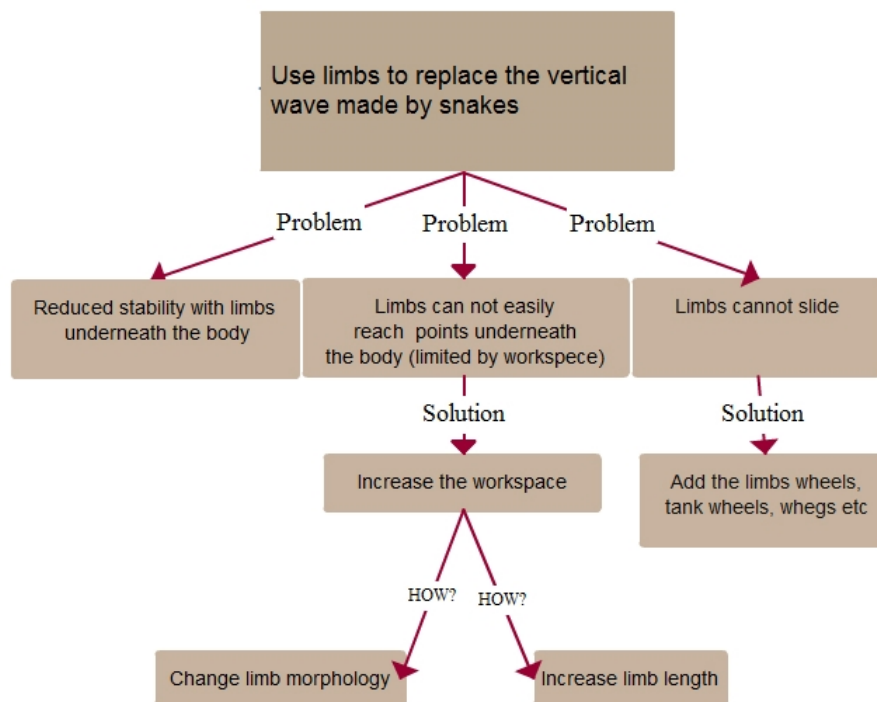


Figure 5.1.: Use Pleurobot’s limbs to replace the vertical wave of snakes

The vertical wave can be easily produced by the spine of Pleurobot. However, using the limbs to reproduce the vertical wave that makes the body redistribute its own weight to a new GCT is not straight-forward.

First of all, for the side-winding gait to be as close as possible to the one of the snakes the ground contact points have to be under the spine, which involves that the limbs should be placed in those respective points. However, considering the workspace of the limbs, and the positions of the joints necessary to reach points under the spine, that is practically impossible.

There are several major problems for which this is impossible. One of them is reduced stability. This happens because as the end tips of the limbs get closer to the ground footprint of the spine, the polygon sustaining the robot is reduced which leads to a decrease in stability. Then, there is the problem of reduced workspace. However, there might be ways of increasing the workspace and solve it: the workspace can be increased by increasing the limb length or changing completely the morphology. However, we did not further explore this solution. Thirdly, even if the robot would be stable with the limbs underneath the spine and the workspace would allow that, there is another mechanical limitation that the Pleurobot cannot overpass: the snakes lay and lift their bodies on the ground. The Pleurobot would have to use its limbs to slide, and it is not the case. Figure 5.1 sums up all this discussion.

After discussing this first approach, it is easy to already conclude that not all the features in the snake's way of producing the gait can be ported to the salamander robot. That is why, the idea of using a vertical wave and slide or propagate the limbs was left behind. Then, some new approaches were considered, while using the limbs to produce a walking-like gait, but coordinated with the spine's sinusoidal wave. These approaches are detailed in the following sections.

5.2. Using a State Machine

5.2.1. The Method

The idea of using a State Machine withholds the fact that the limbs should be coordinated among each other, while also coordinating with the spine. The coordination between the spine and the limbs is highly important as it ensures a faster locomotion. This was observed in *Biorob* on *Salamandra Robotica* for forward locomotion (<http://biorob2.epfl.ch/utills/movieplayer.php?id=34>).

As the timed horizontal and vertical waves are helping the sand snakes have a fast locomotion, it is also important to have it synchronized with the limbs in the Pleurobot's side-winding.

Static Cartesian trajectories having an established number of points are generated and by using Inverse Kinematics the joint trajectories are generated.

The designed state-machine has 4 states in which the front left (FL) and right hind (HR) limbs are pushing/pulling in one direction while the front right (FR) and hind left (HL) are in the swing phase. When the FL and HR finish the stand state, they enter the swing phase and the complementary limbs start the stand state. These two states are

done for lateral displacement, but their resulting motion is on the direction of the GCT's, which leads to an overall, diagonal displacement. To compensate for the backwards diagonal displacement each limb has two more states in which a small correctional frontal displacement is made. In short, the exact state-machine functions as illustrated in Figure 5.2.

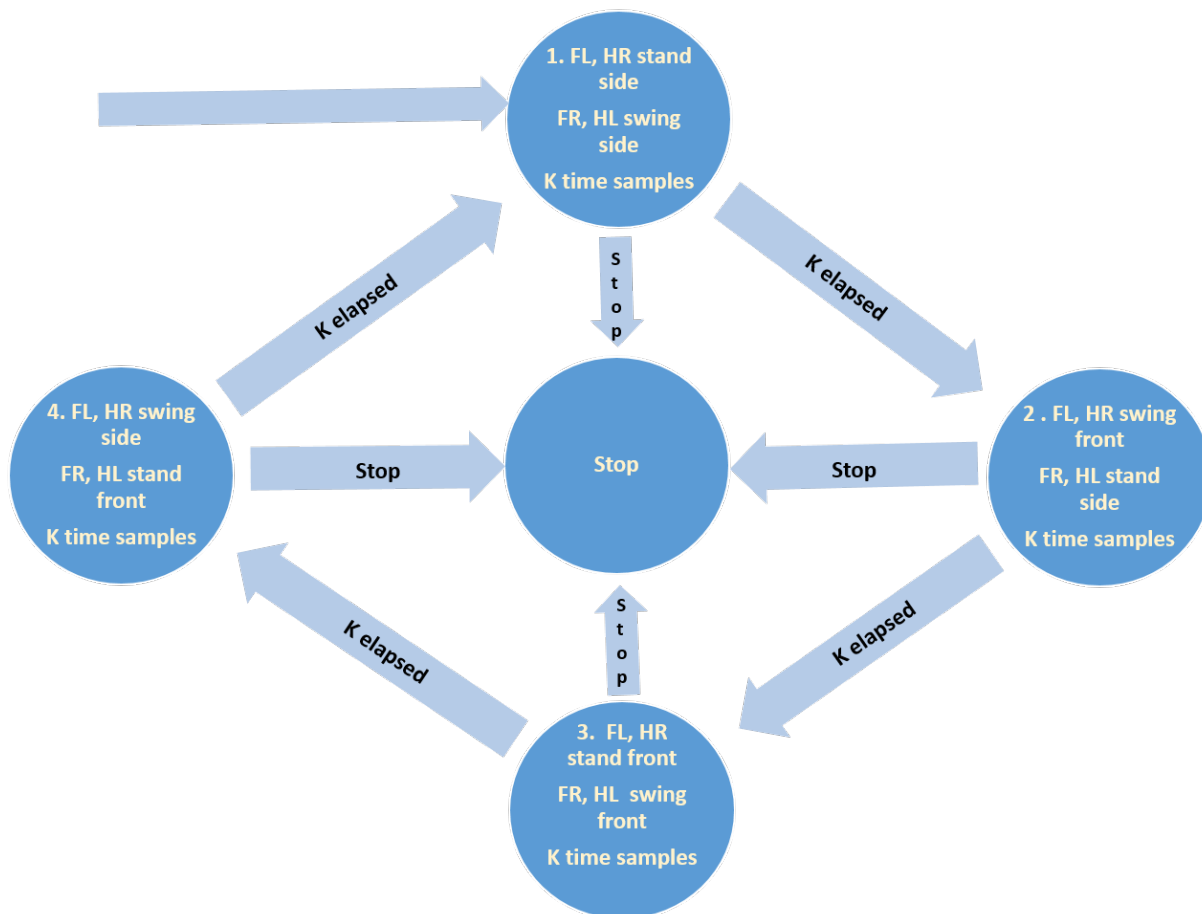


Figure 5.2.: The chart shows the four states of a finite state machine that describes the logic behind the side-winding implementation that was used

This approach has proved to have various inconvenient features. First of all, the motion of limbs is independent of the spine motion so they have to be statically designed to coordinate. Then, while the limbs are performing their trajectory, the spine is also advancing. To that it adds the fact that the trajectories are defined in the robot's frame of reference (RFOR). In the case of moving to the right, this leads to a part of left limbs' trajectories not be reachable because they get out of the workspace, and a part of right limbs' trajectories get very close to the spine. The results is an undesired overall motion (or instance the elbows hitting the floor), self collisions (between the limbs and the spine) and various singular positions. Figure 5.3 depicts a chart with problems and solutions of this approach.

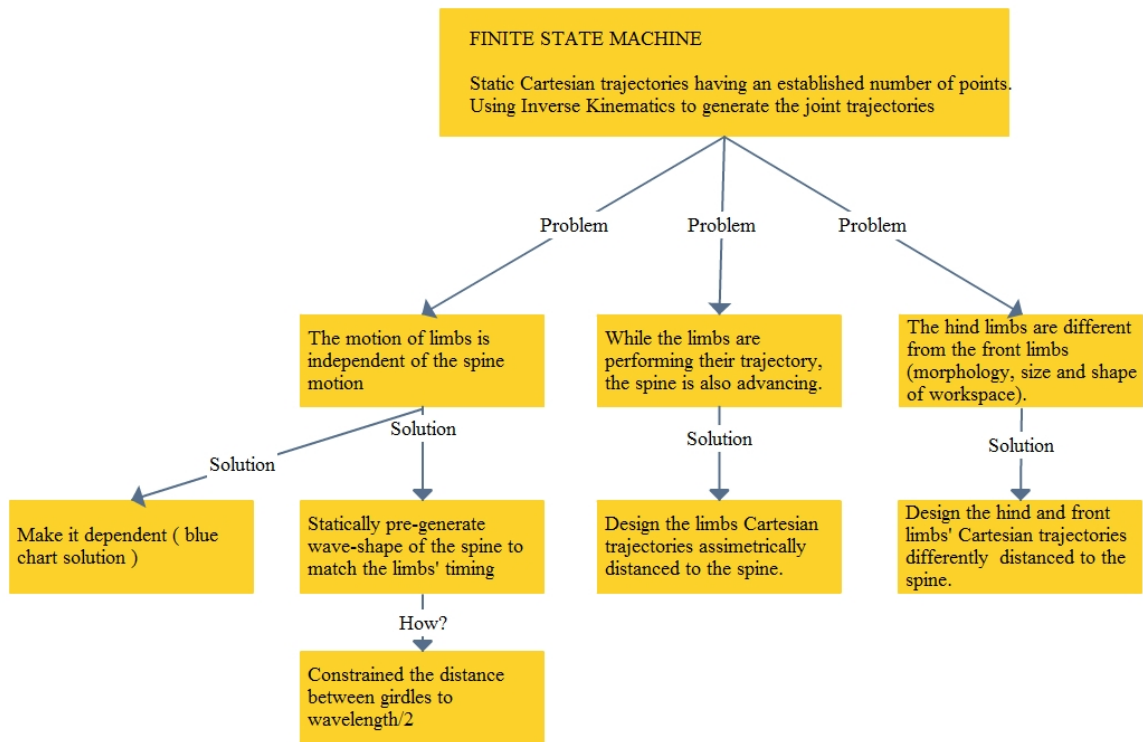


Figure 5.3.: The chart presents different aspects related to the *State Machine* approach

5.2.2. Tests

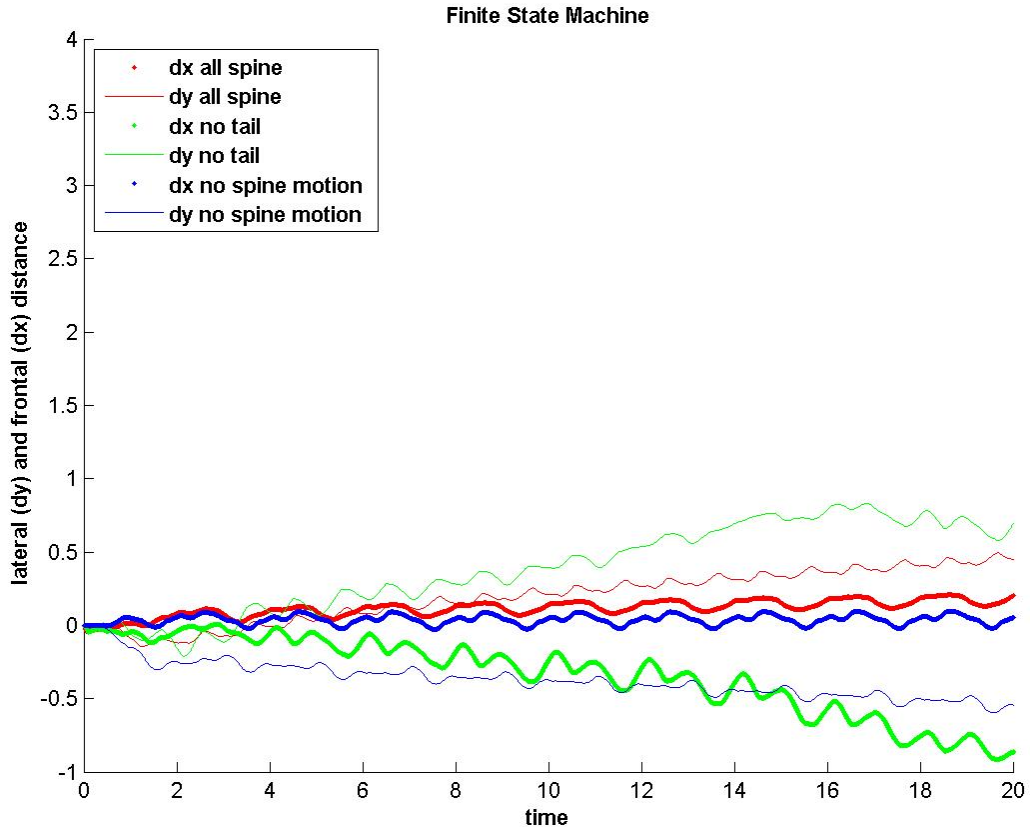
The State Machine was implemented in Matlab. Once the Angles were generated, they were tested first in a Matlab simulation of Pleurobot and then in Webots. The trajectory in time of the front and hind girdles was monitored with GPS's and saved.

Figure 5.4 a) shows a comparative plot of the evolution of the trajectory on x and on y in time for the cases in which all spine is used (red), the tail is inactive (green) and the spine is not used at all (blue). It gives a good description of speeds and directions of the approach. For side-winding it is desirable that the displacement occurs only on the y axis.

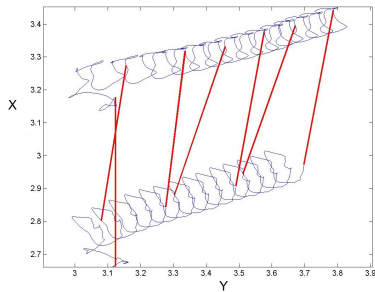
Remark: In charts 5.4 a), 5.7 a), 5.8 a) and 5.10 a) the y value has the opposite sign with the purpose to avoid unaesthetic overlapping of plots.

As it can be seen, the biggest displacement on y is represented by the thin green line, which represents the case with no tail, but it can also be seen that it also has the biggest displacement on x , which is not quite desired. The case with all spine and tail used seems to be the best because it has the biggest displacement on y and almost no displacement on x .

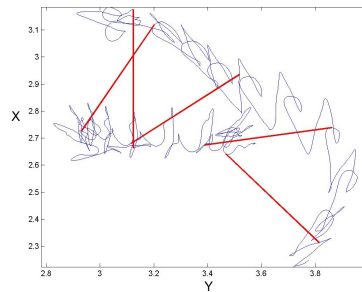
a) Comparative view



b) Using all spine and tail



c) Not using tail



d) Not using spine at all

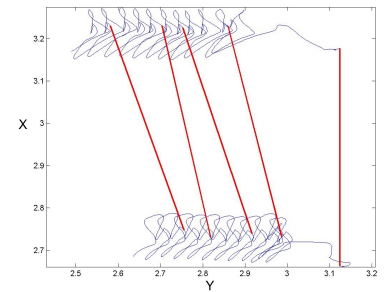


Figure 5.4.: Chart a) presents a comparative view of the displacement on x and y (desired) axis in time for the cases in which the robot has **all the spine enabled (red)**, has the **tail disabled (green)**, or does **not use the spine at all (blue)**. The smaller images are showing how the orientation of the robot is changing in time: b)-using all spine, c)-disabling the tail and d)-not using spine at all. It can be observed that in case c) when the tail is disabled, but the spine is still undulating, the orientation suffers a big deviation from the normal case.

Apart from the direction of displacement and speed, it is also interesting to see how the orientation of the robot changes in function of using or not using the spine. Figure 5.4 b)-using all spine, c)-disabling the tail and d)-not using spine at all show in red the RFOR. It can be observed that for the case in which all spine is used maintains the spine aligned with its initial position.

5.3. Have a "Spine-Triggered" Motion of The Limbs

5.3.1. The Method

The idea of using a state machine to coordinate the limbs' motions has proved to have the drawback that the states of the four limbs and spine were pre-defined and the wave function of the spine had to be defined in such a way that in all the states it will be coordinated with the positions and motions of the limbs to help maximize the displacement that they do.

A potentially better approach was considered to decide to make the steps (on pre-defined trajectories w.r.t. the robot's frame of reference and use inverse kinematics) when the sine function in the spine is reaching a maximum in the direction of displacement (or a minimum in the opposite direction). The drawbacks of this method can be observed in the condensed schema in figure 5.5.

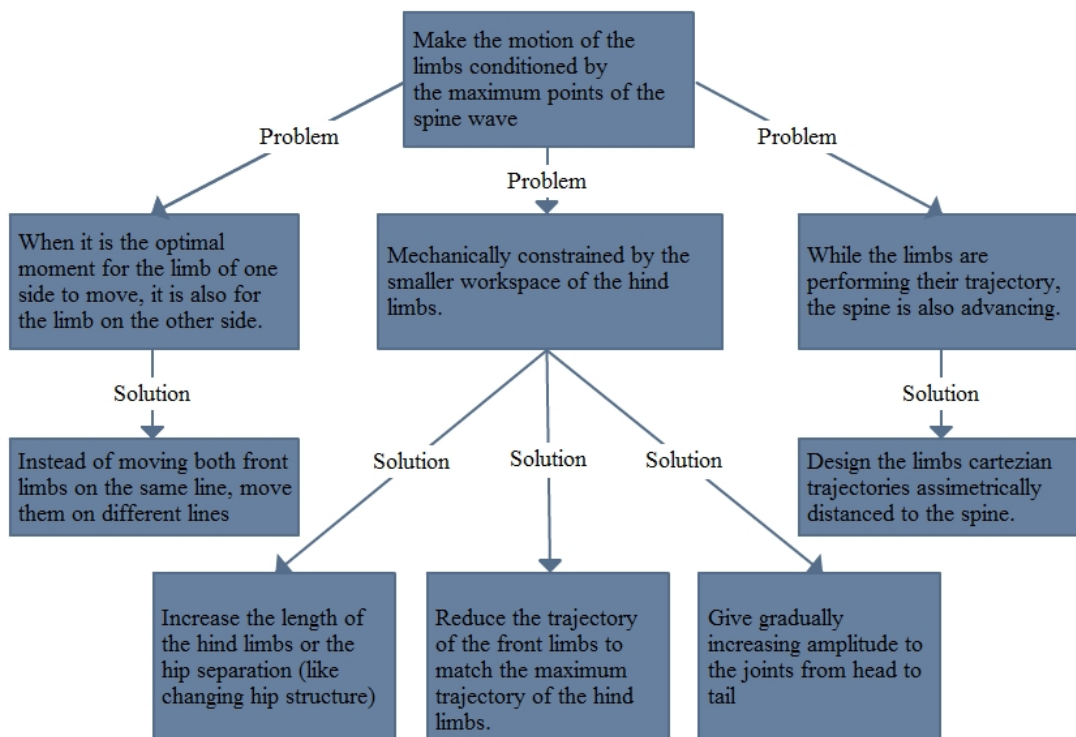


Figure 5.5.: The chart presents different aspects related to the *Spine-Triggered* approach

One drawback is that, unlike the case of forward displacement, while a peak (maximum amplitude) of the spine on the side of displacement, and thus a good moment to place a step with the respective limb, it is also the right moment for the other side's limb to step. The solution to that is to change the levels of the trajectory on the x axis as shown in Figure 5.6 c). However, this, as well, does not provide a perfect motion because while the limbs follow their trajectories the spine is also advancing on the y axis, thus, reducing modifying the workspace on both sides of the robot. The solution is depicted in Figure 5.6 d) where the trajectories to be followed are not symmetric with respect to the body's axis. as shown in Figure 5.6 a) and b)

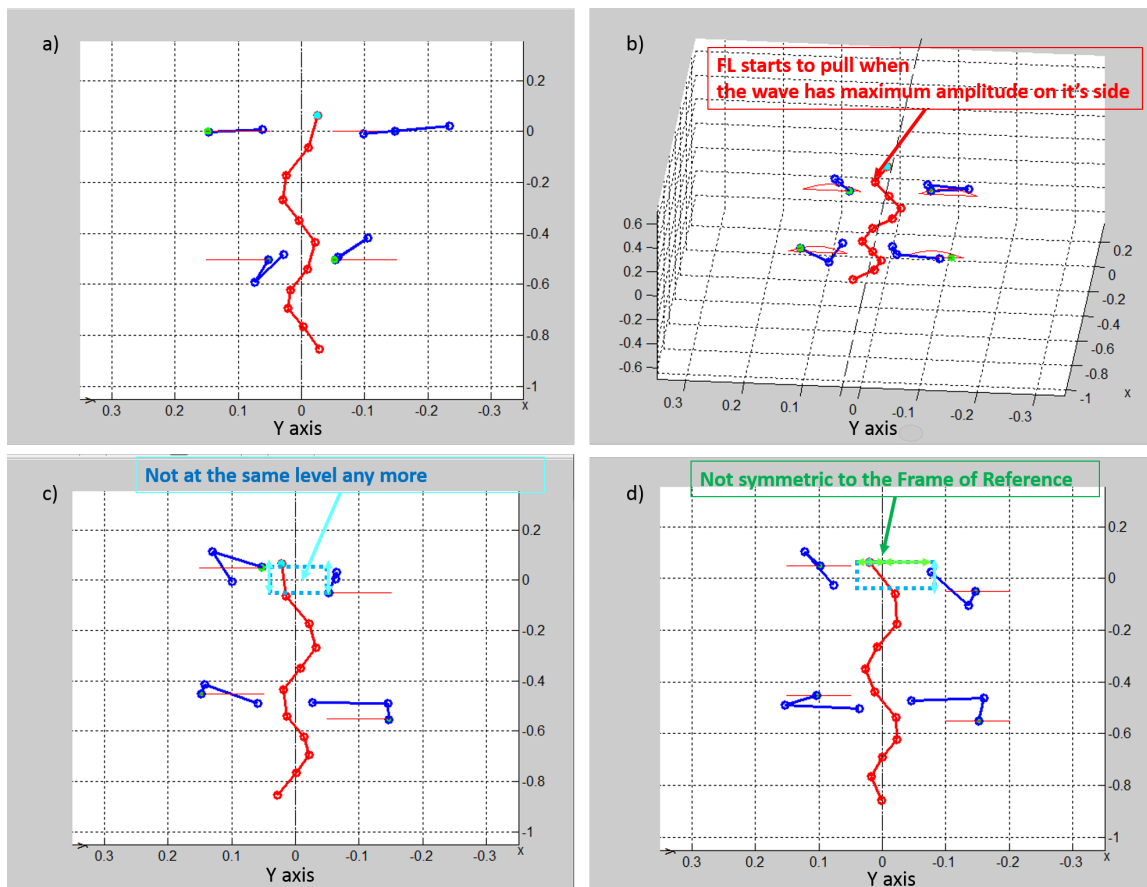


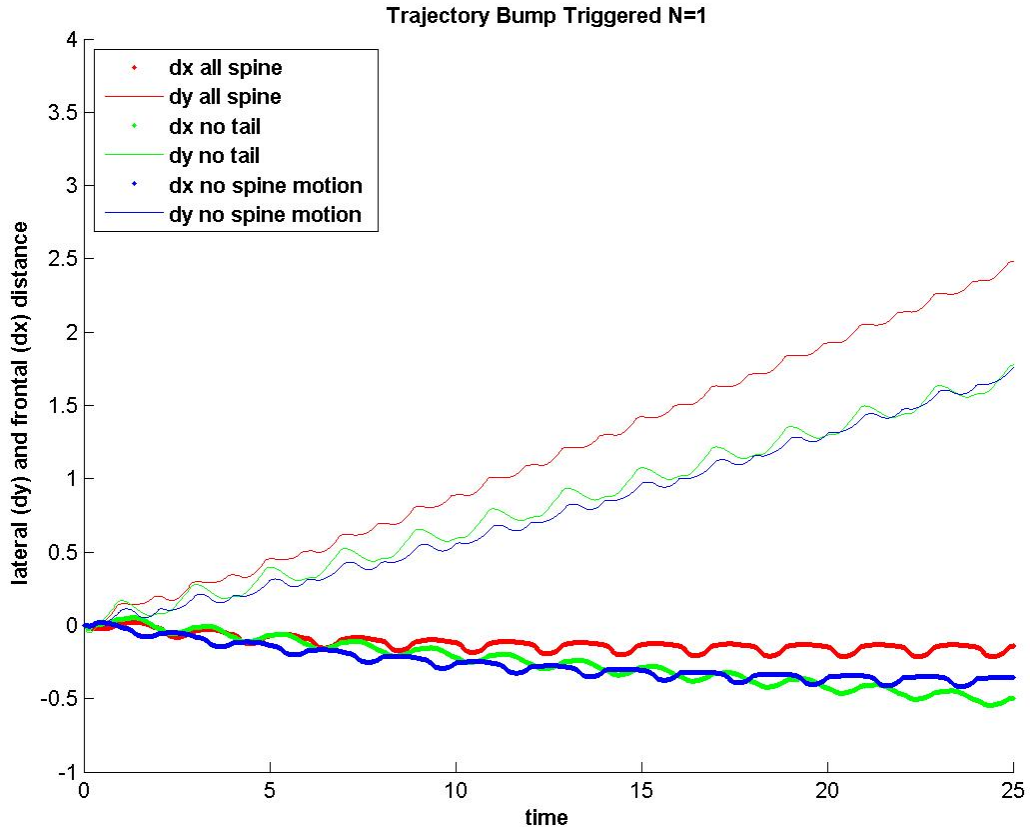
Figure 5.6.: The chart presents different variations of the "Spine-Triggered" method

5.3.2. Tests

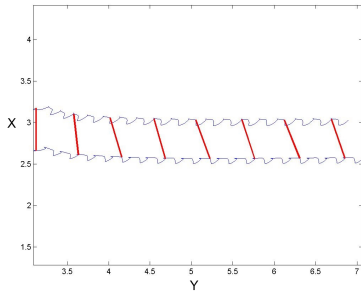
As in the case of the state machine, the code generating spine-triggered movements of the limbs was implemented in Matlab and once the angles generated, the motions could be observed in a Matlab animation and in Webots. Similarly, GSPs, mounted on the front and hind girdle in the Webots simulation to track the trajectories and orientations of the robot throughout different simulations, with the purpose of making qualitative evaluations of the gait in different situations.

First of all, the gaits were ran for the case with all the spine used, no tail used, and no spine at all used. For this comparative set of experiments, the joints of the spine and limbs had the same speed (the frequency of the spine is fixed, but while the spine function performs one cycle, the limbs also do their pre-established trajectory once). Then, after this experiment the case with all the spine used was chosen and a new set of experiments was done, for different ratios of the speed between the spine and the limbs.

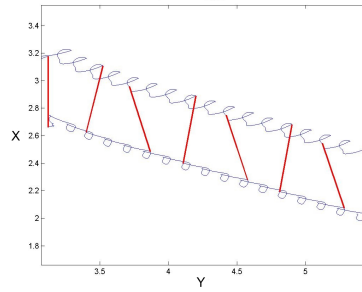
a) Comparative view



b) Using all spine and tail



c) Not using tail



d) Not using spine-tail at all

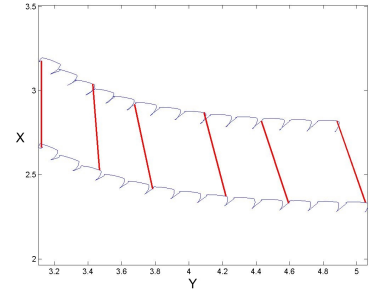
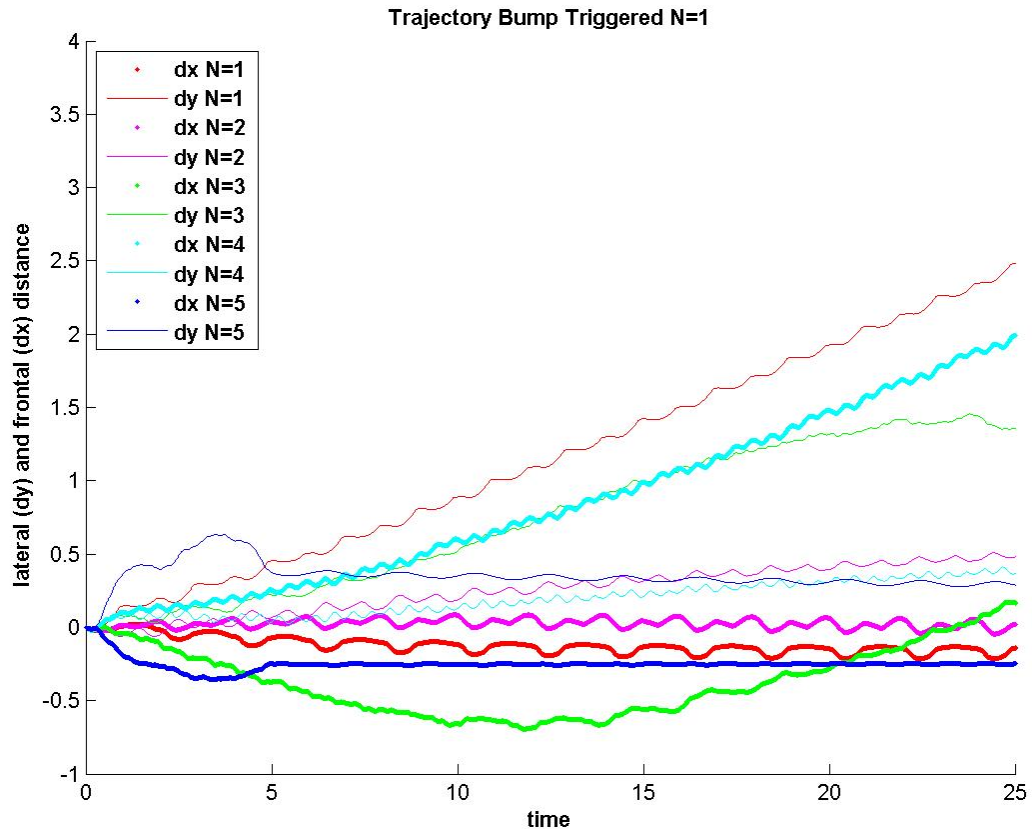


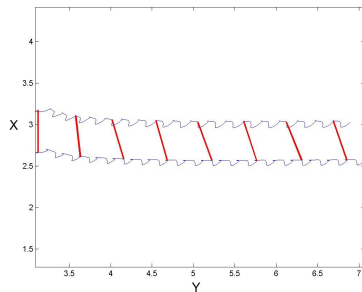
Figure 5.7.: The images present the speed, trajectories and orientation of the robot for the case in which the spine's and limb's joints move at the same speed. Chart a) presents a comparative view of the displacement on x and y (desired) axis in time for the cases in which the robot has **all the spine enabled (red)**, has the **tail disabled (green)**, or does **not use the spine at all (blue)**. The smaller images are showing how the orientation of the robot is changing in time: b)-using all spine, c)-disabling the tail and d)-not using spine at all. It can be observed that in case c) when the tail is disabled, but the spine is still undulating, the orientation suffers a big deviation from the normal case

In Figure 5.7 a) it can be observed that the biggest displacement on y and the smallest displacement on x is done in the case in which the spine and tail are used. Images 5.7 b)-d) confirm that the displacement is strictly lateral and that the orientation of the robot does not change for the case in which all the spine is used. Therefore, to analyze the influence of the speed ratio between tail and limbs, only for the the case of all spine and tail experiments were conducted.

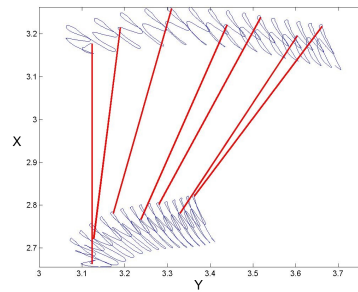
a) Comparative view



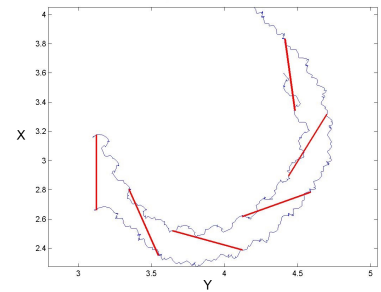
b) Ratio=1



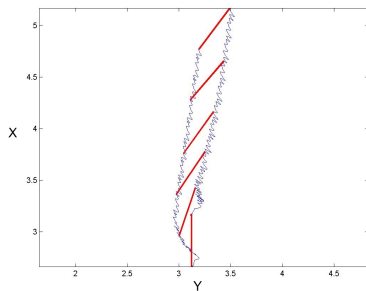
c) Ratio=2



d) Ratio=3



e) Ratio=4



f) Ratio=5

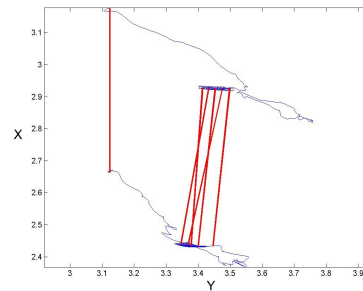


Figure 5.8.: The images present the speed, trajectories and orientation of the robot for the case in which the spine's and limb's joints move at different speeds ratios. Chart a) presents a comparative view of the displacement on x and y (desired) axis in time for the cases in which the robot has all the spine enabled for speed ratios between spine and limbs spanning from 1 to 5. The smaller images are showing how the orientation of the robot is changing in time: b) ratio 1, c) ratio 2, d) ratio 3 e) ratio 4 and f) ratio 5.

This experiment was conducted to check the effect of increasing the speed of the limbs relative to the speed of the spine. Ratio 5 means that the limbs are performing 5 closed trajectory w.r.t. the RFOR while the spine is only performing one. It was interesting to check this because as **Melo; 2015** shows, there is a value of the resulting speed of the gait, equal to $V_{net} = \omega\lambda L \tan\rho$ dependent on the speed of the wave propagation. At $ratio = 1$ the limbs (the analogue of the vertical wave of the snakes) of the snakes did not seem to be "propagating" with the same speed as the spine. However, as images 5.8 a) shows, the fastest displacement is for $ratio = 1$. As well, it also ensure the least trajectory and orientation deviation.

5.4. Stabilize the Girdles and Compute the Joints Angles from Wave Functions

5.4.1. The Method

The previously presented approaches involve predefined trajectories to be followed by the limbs and inverse kinematics that sometimes brings them in unnatural positions, or sometimes even fails to bring the limbs to following the designed trajectories.

In the case of Lola-OP 16-DOF snake modular robot the output angles are not the result of inverse kinematics, but of the two wave functions presented in 2.1 that directly provides the angles $\Theta(n, t)$ that need to be provided at every moment t to every joint n . Since this was successfully implemented in Lola, it was worth trying it for Pleurobot. As before, the spine function was a sinusoidal one, having half a wavelength between the girdles.

Then, the angles made by the girdles with the robot's frame of reference were measured. Having these angles, the *Yaw* actuators were corrected with it, and then, to it, the angle corresponding to the correct direction of the side-winding gait was added. This way, both girdles were aligned with the correct GCTs to be followed, represented by an angle ρ . After that, the *Pitch*, *Roll* and *Knee-Elbow* were successively added to build the final desired trajectory. Different aspects of the approach are summarized in Figure 5.9.

Limbs vs. gaits	Yaw	Pitch	Roll	Knee-Elbow
Front Left	Front Girdle compensation $-\rho$	Equation 5.1	$\pi/2$	Θ_{Elbow} in Equation 5.2
Front Right	Front Girdle compensation $-\rho$	Equation 5.1	$\pi/2$	$-\Theta_{Elbow}$
Hind Left	Hind Girdle compensation $-\rho$	$0t$	$0t$	$-\pi/2$ $-$ $scale\Theta_{Elbow}$
Hind Right	Hind Girdle compensation $-\rho$	$0t$	$0t$	$\pi/2$ $+$ $scale\Theta_{Elbow}$

Table 5.1.: Summary of the angles that have to be commanded directly to the joints

$$\Theta_{Pitch}(t) = A_{Pitch} \sin(\omega t + \Phi_{Pitch}) \begin{cases} A_{Pitch} = \pi/18; \\ \Phi_{Pitch} = \pi/4; \end{cases} \quad (5.1)$$

$$\Theta_{Elbow}(t) = -A_{Elbow} \text{Sin}(\omega t + \Phi_{Elbow}) \begin{cases} A_{Elbow} = 3\pi/18; \\ \Phi_{Elbow} = \pi/4; \\ scale = 0.55. \end{cases} \quad (5.2)$$

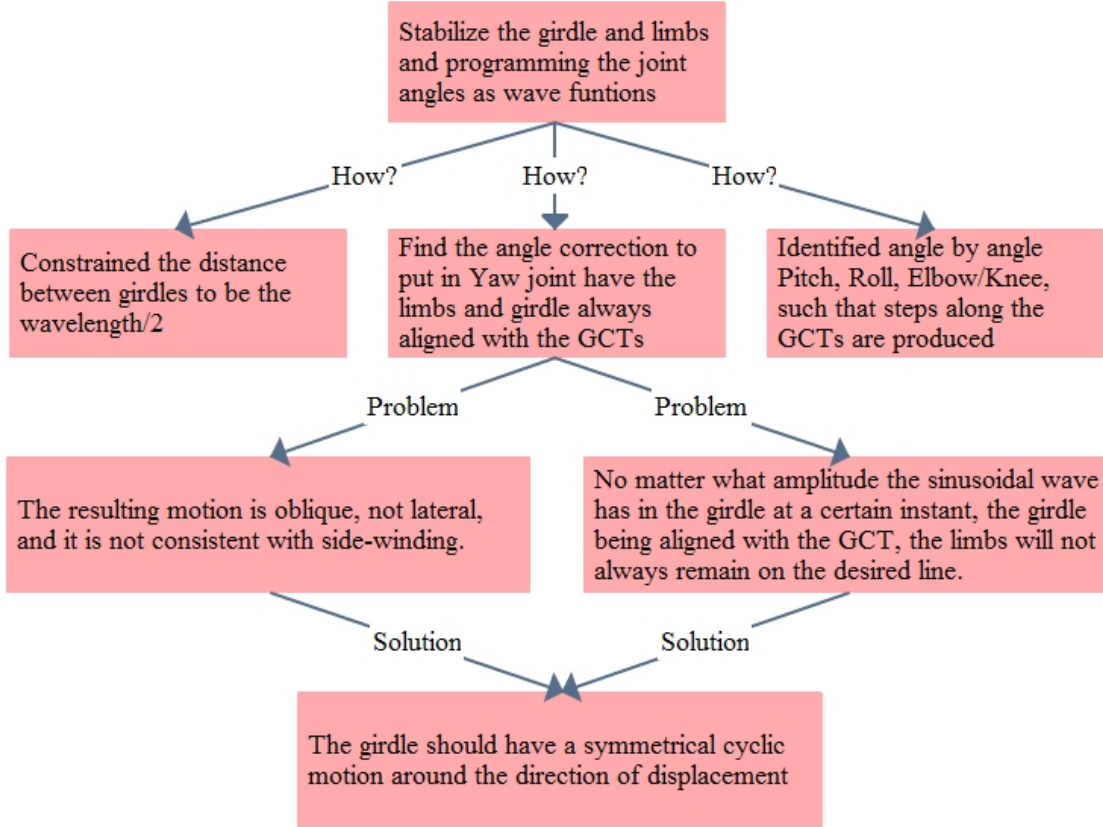


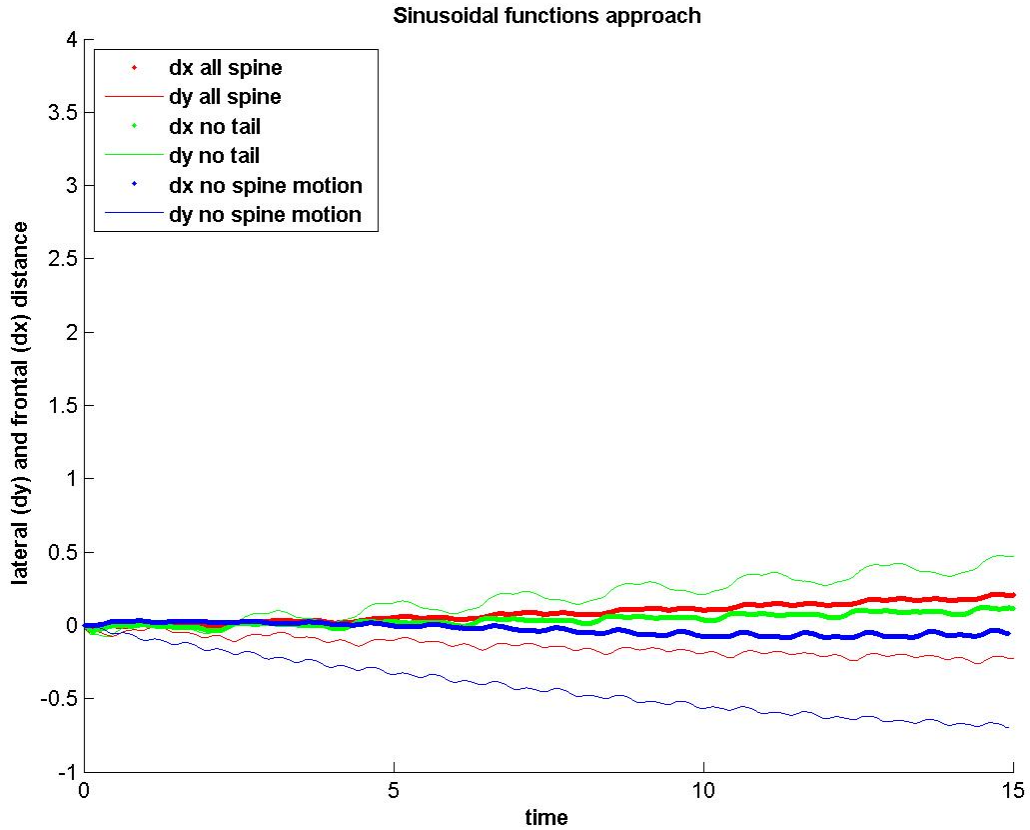
Figure 5.9.: The chart presents different aspects related to the Wave Functions approach

5.4.2. Tests

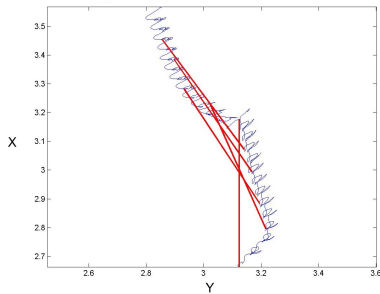
Unlike in the previous approaches, where the angles were generated by inverse kinematics, this time the angles inputted to the robot are inputted directly as previously explained.

In the previous cases, the best choice was to use all the tail, figure 5.10 suggests that not using tail is the best choice in terms of speed. Furthermore, the orientation of the robot is better maintained when the spine is used, but the tail is disabled.

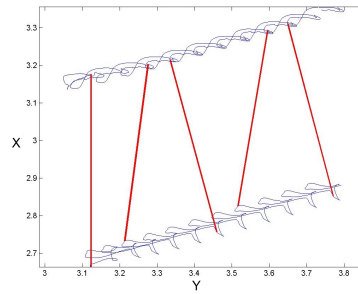
a) Comparative view



b) Using all spine and tail



c) Not using tail



d) Not using spine-tail at all

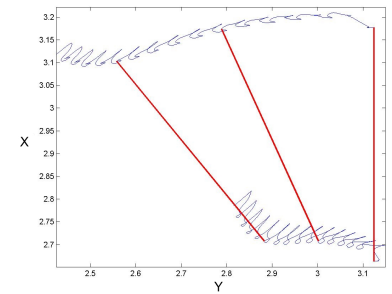


Figure 5.10.: The images present the speed, trajectories and orientation of the robot for the case in which the spine's and limb's joints move at the same speed. Chart a) presents a comparative view of the displacement on x and y (desired) axis in time for the cases in which the robot has all the spine enabled (red), has the tail disabled (green), or does not use the spine at all (blue). The smaller images are showing how the orientation of the robot is changing in time: b)-using all spine, c)-disabling the tail and d)-not using spine at all. It can be observed that in case c) when the tail is disabled, but the spine is still undulating, the orientation suffers a big deviation from the normal case

5.5. Comparing The Methods

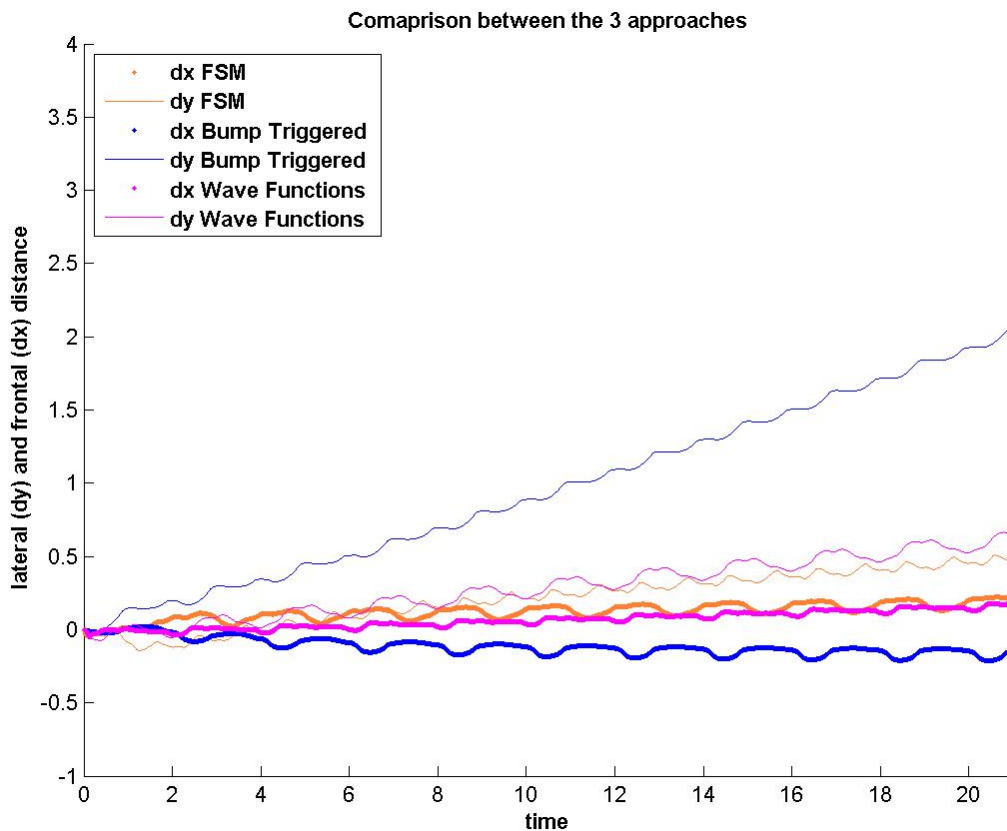
Here, the most promising gaits of each approach is compared in order to establish which method of replicating the snake's side-winding in Pleurobot is the most effective. The

comparison is made in terms of speed, deviation of direction and orientation of the RFOR, based, as previously, on the GPS data recorded in Webots.

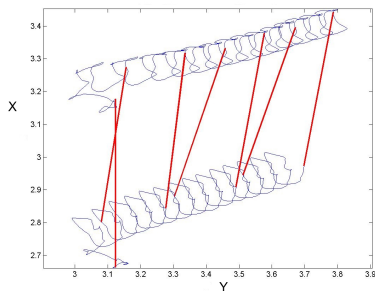
Looking at Figure 5.11, it is the second approach which is the in terms of speed and maintaining the orientation of the body. Figure 5.11 a) shows that the speed of the "Peak-Triggered" approach is a lot bigger than the other two. However, this does not necessarily mean that the other two approaches are a lot worse, since there are many parameters that were not tuned or explored during the implementation, as the purpose of this project was not parameter tuning, but rather exploring different types of gaits.

Another important remark is that to the implementation of the "Peak-Triggered" algorithm for generating angles, was added the girdle correction done by the *Yaw* joint. So, in comparison to the worse methods, the one based on the maximum amplitude of the sinusoidal function and side walk is also more thoroughly implemented than the others.

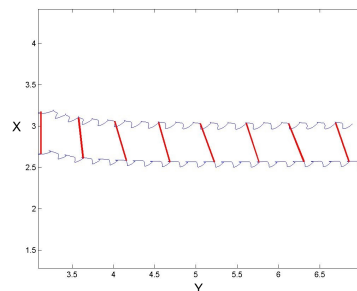
a) Comparative view



b) Using all spine and tail



c) Not using tail



d) Not using spine-tail at all

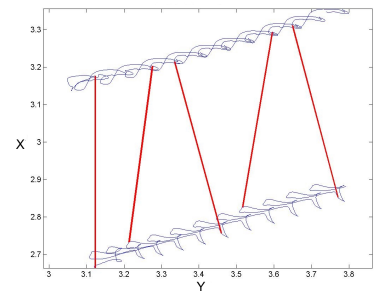
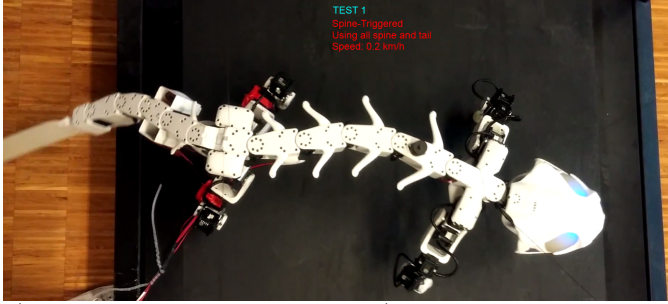


Figure 5.11.: Comparative view between the best gait of each designed method

5.6. Practical Experiments

In order to make tests on the real Pleurobot, the robot was suspended with ropes on a running treadmill, with the purpose to protect it and to make the tests easier. Four different sets of angles were chosen, considered to be the least likely to harm the robot, according to Webots simulations. Therefore, the tests were performed for the Spine-Triggered approach with all spine and tail used (Figure 5.12 a) , with spine and without tail (Figure 5.12 d)), for the State Machine using all spine and tail (Figure 5.12 c)), and just stepping side (Figure 5.12 b)).

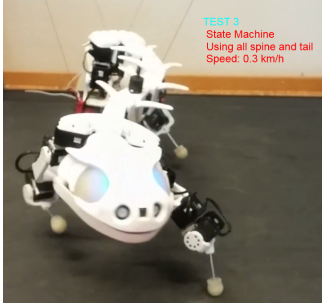
a) Test 1



b) Test 2



c) Test 3



d) Test 4

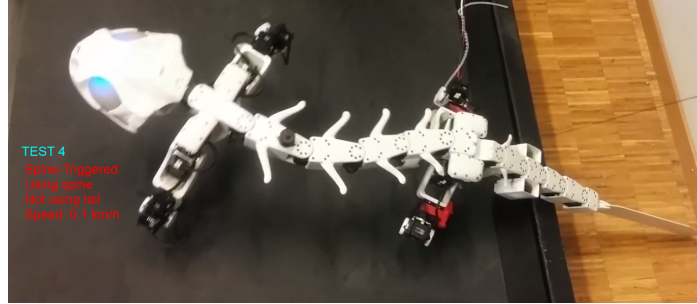


Figure 5.12.: Tests on Pleurobot

All tests proved very small speed: $0.1\text{-}0.2\text{ km/h}$ for the Spine triggered approach and the test with no undulation, and 0.3 km/h for the state machine. The speed of locomotion was measured by letting the salamander walk and gradually increasing the treadmill's speed.

The results are contrasting with the ones presented in the previous section, and which were based on data provided by Webots. However, if all the parameters of the gait are considered, the results are not quite surprising: for the implementations, low, but different amplitudes of the spine were used in order to avoid internal collisions. More precisely, for tests 1, 2, and 4 the used parameters were $A = \pi/9$, $\lambda = 1$, and $\omega = 2\pi$, while for the state machine (test 3), the values were $A = \pi/6.3$, $\lambda = 1$, and $\omega = 4\pi$. Therefore, the results prove the high importance of the spine's amplitude and frequency. Still, the differences between simulations and real robot might also be due to the fact that the robot was not actually walking, but hanged, even if the limbs were touching the ground. As well, the friction with the treadmill is a factor that was not taken into account in the simulations. Finally, more forces interfered as the treadmill's surface was not large enough to completely fit on it, but the tail was slightly hanging outside.

6. Conclusions and Further Work

Various manners of porting the side-wing gait from snake-robots to Pleurobot were discussed, implemented and tested. As a result, there are several conclusions that are worth listing.

First of all, in many of the cases presented in Chapter 5, the orientation of the robot was gradually changing (Figures 5.4 c), 5.7d), 5.8c) and d)), while the trajectory was deviating in a curvilinear shape. This is somehow consistent with the concept of "conical side-winding" briefly presented in Chapter 2, Section 2.1.3. This might be due to several factors like for instance friction caused by the tail, hind limbs different from the front ones, and especially unequal size of the spine modules of the robot (which induces unequal amplitudes in the wave). For simplicity, it was considered the generalization that all the vertebraes are equally sized. The difference in size leads to variations in the amplitudes along the spine's wave, which is equivalent to inducing a conical side-winding. This might be corrected by using a wave function with variable amplitudes throughout the different joints.

An interesting observation was done in the case of the Wave Functions method (Chapter 5, Section 5.4). Reversing the frequency of the waves reverses the direction of displacement. This is similar to the case of the lamprey vertebrate, in which, if the sinusoidal wave is propagated in the opposite direction (tail-head), it swims backwards. Another similarity between Pleurobot and lamprey is that while the frequency of the spine wave can be changed, the wavelength cannot. In order to ensure efficient motion, it is important to have half of a wave between the two girdles.

Furthermore, it was observed that not only the portion of the spine between the girdles is important in locomotion, but also the tail, which may drag in a useful or harmful direction. Therefore, the tail is an important parameter to consider in the case of side-winding, and, in most cases, it should be used.

It was also noticed that increasing the speed of the limbs while leaving unchanged the speed of the spine wave, declines the locomotion and suggests once again that the spine and the limbs should always be coordinated (as shown in 5.3.2).

Finally, as Figure 5.11 a) showed, the speed of the "Peak-Triggered" approach is a lot bigger than the other two, thus making this approach the best competitor *so far* for the side-winding gait in Pleurobot. The other methods presented in chapter 5 might also lead to good results if perfected and finely tuned.

A further direction to which this research topic might be directed is changes in the robot's design, like adding extra limbs to improve stability and allow more complex motions. A change that would allow the Pleurobot to become a better side-winder might be adding it wheels at the limbs' tips. This would enable slipping that might replace the snake's bodies strategy on laying and peeling their bodies off the ground. Another morphological change that would enhance it's side-winding possibilities would be to have a few (maybe 5) of the 11 joints of the spine with the capability of vertical bending.

Finally while porting the side-winding gait to Plerobot can be done in various ways, it is difficult to reproduce the speed and elegance of snakes in a quadruped robot. However, the most important observation is that the traveling wave present in the Pleurobot's spine is beneficial for side displacement because the amplitude of the wave itself adds up to the displacement performed by the limbs.

Bibliography

- [1] J. Burdick, J. Radford, and G. Chirikjian, "A "Sidewinding" Locomotion Gait for Hyper-redundant Robots," *Robotics and Automation*, vol. 3, pp. 101-106, 1993.
- [2] R. L. Hatton and H. Choset, "Sidewinding on slopes," in *Proceedings of the IEEE International Conference on Robotics and Automation*, Anchorage, AK USA, May 2010, pp. 691-696.
- [3] C. Gong, R. L. Hatton, and H. Choset, "Conical sidewinding," in *Robotics and Automation (ICRA), 2012 IEEE International Conference on, may 2012*, pp. 4222-4227.
- [4] K. Melo, "Modular Snake Robot Velocity for Side-Winding Gaits," in *Robotics and Automation (ICRA), 2015 IEEE International Conference on, may 2015*.
- [5] Hamidreza Marvi, C. Gong, N. Gravish, H. Astley, M. Travers, R. L. Hatton, J. R. Mendelson III, H. Choset, D. L. Hu, D. I. Goldman, "Sidewinding with minimal slip: Snake and robot ascent of sandy slopes," in *Science Magazine, VOL 346 ISSUE 6206, on 10 OCTOBER 2014*
- [6] Shigeo Hirose, Hiroya Yamada, Snake-like robots [Tutorial], *IEEE Robot. Automat. Mag.*, volume 16, number 1, pages 88-98, 2009,
- [7] Auke Jan Ijspeert, Computational Motor Control Lectures, Lecture 4, 2015
- [8] <http://biorob2.epfl.ch/utils/movieplayer.php?id=34>

Appendices

A. Notations And Acronyms

GCT = abbreviation that stands for "Ground Contact Tracks";

GCS = abbreviation that stands for "Ground Contact Segments";

AS = abbreviation that stands for "Arch Segments";

DOF = abbreviation that stands for "Degrees of Freedom";

FOR = abbreviation that stands for "Frame of Reference";

RFOR = abbreviation that stands for "Robot's Frame of Reference";

GFOR = abbreviation that stands for "Global Frame of Reference";

FL = front left limb of Pleurobot

FR = front right limb of Pleurobot

HL = hind left limb of Pleurobot

HR = hind right limb of Pleurobot